Chapter 5

Polarized Backlights Using Selective Internal Reflection at Micro-grooves

In the previous chapter, polarized backlights using sub-wavelength grating was introduced. Upon the impingement of unpolarized light on the sub-wavelength grating, only p-polarized light was transmitted while s-polarized light was reflected. S-polarized light was then converted into p-polarized light by passing through the quarter wave plate twice. Therefore, extracted light became uni-polarized. However, by using e-beam lithography, the cost of the sub-wavelength grating hinders its application. Additionally, the area of the sub-wavelength grating is small, which is limited by the e-beam writer. Consequently, in **Chapter 5**, we proposed a novel polarized backlights using selective total internal reflection (T.I.R). Polarization separation within the lightguide by selective T.I.R at an isotropic substrate-anisotropic layer was combined with a subsequent separate light outcoupling of the linearly polarized light at a micro-machined groove structure.

5.1 Principle of Polarized Backlights Using Selective T.I.R

Polarization backlight based on selective Total Internal Reflection (T.I.R) at the interface of micro-structures was schematically shown in Fig. 5-1.[1] An anisotropic layer with micro-grooves was filled with an isotropic index-matching layer, adhered to the lightguide substrate. The anisotropic layer has an ordinary index of refraction, n_o, which is closely matched the refraction index of index-matching layer and an extraordinary refraction index, n_e. The approach to separate the polarized

light was aimed to extract one polarization state of light by selective T.I.R at the micro structure interface. The extraordinary refractive index n_e of the anisotropic layer should be significantly larger than the refractive index n_c of index-matching layer to achieve a sufficiently small critical angle at the interface. In contrast, the critical angle at the interface is not present for the orthogonally polarized light. Light therefore remains its propagating direction at the interface of micro-structures.[2][3]

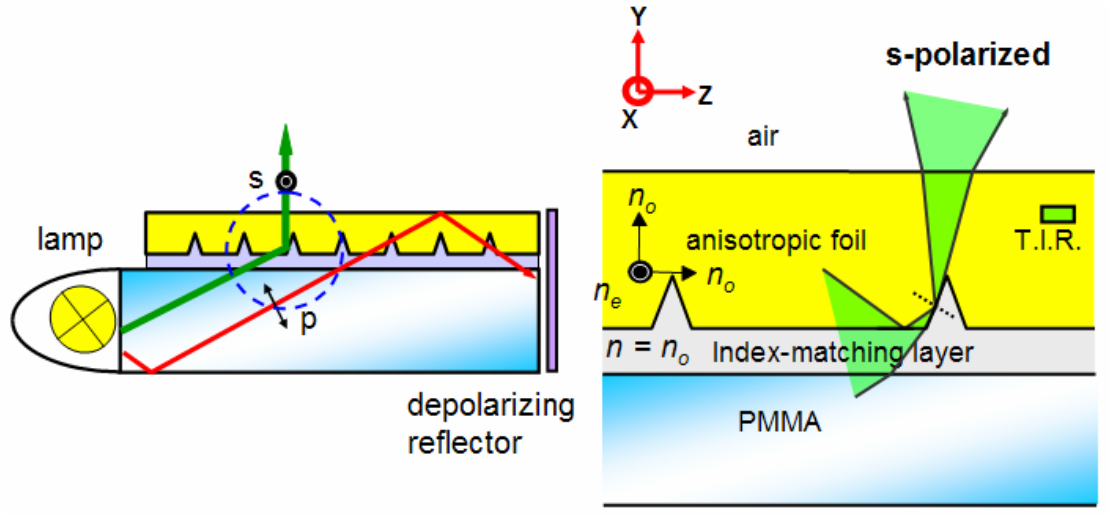

Fig. 5-1. Schematics of polarized backlight. Birefringent layer with micro grooves filled with index-matching layer was aimed to extract the s-polarized light at the interface. Additionally, p-polarized light was trapped in the polymethyl methacrylate (PMMA) lightguide to be recycled.

5.2 Theory of Selective T.I.R at Micro-grooves

The electric field amplitude E can be decomposed either parallel or perpendicular to the incident plane. The transmission coefficient t and reflection coefficient r depend on the incident polarization direction and are given by the Fresnel equations for dielectric media:[4][5]

TE (s-polarization): $t = \frac{E_t}{E} = \frac{2\cos\theta_i}{\cos\theta_i + \sqrt{n^2 - \sin^2\theta_i}}$ (5-1)

TM (p-polarization): $t = \frac{E_t}{E} = \frac{2n\cos\theta_i}{n^2\cos\theta_i + \sqrt{n^2 - \sin^2\theta_i}}$ (5-2)

TE (s-polarization): $r = \frac{E_r}{E} = \frac{\cos\theta_i - \sqrt{n^2 - \sin^2\theta_i}}{\cos\theta_i + \sqrt{n^2 - \sin^2\theta_i}}$ (5-3)

TM (p-polarization): $r = \frac{E_r}{E} = \frac{n^2\cos\theta_i - \sqrt{n^2 - \sin^2\theta_i}}{n^2\cos\theta_i + \sqrt{n^2 - \sin^2\theta_i}}$ (5-4)

in which n is the relative refractive index (=n_2/n_1)

The transmittance T and reflectance R are related to the transmission and reflection coefficients by:[4][5] $T = n\frac{\cos\theta_t}{\cos\theta_i}t^2$ and $R = r^2$

The above-mentioned Fresnel equations show a polarization dependence of the transmittance and reflectance at the interface. As shown in Fig. 5-1, for a uniaxial birefringent film, p-polarized light encounters the low ordinary refractive index n_o and s-polarized light a weighted average of n_o and n_e. The polarization separation can be achieved at the interface by a complete reflection of one polarization direction, where as the orthogonal polarization direction is refracted towards the anisotropic film. Only s-polarized light encounters T.I.R because a critical angle $\theta_c = \sin^{-1}(\frac{n_o}{n_{effective,s-polarized}})$ exits at the interface, where it is extracted from the lightguide. The angular distributions of outcoupling s-polarized light depend on the top angle of micro-grooves in the anisotropic layer.

Fig. 5-2 demonstrates the distributions of s-polarized light if half of the top angle φ is smaller, equal, or exceeding the critical angle $\theta_{c3,4}$ of the anisotropic layer with respect to air.[6] $\theta_{c2,3}$ depicts the critical angle of the anisotropic layer with respect to the index-matching layer. For φ equal or exceeding $\theta_{c3,4}$, light can be refracted at a maximum external outcoupling angle of 90˚ if the incident angle is no more than $\theta_{c3,4}$ at the interface between the anisotropic layer and air. Light is totally

internal reflected and trapped in the lightguide if the incident angle is larger than $\theta_{c3,4}$. For φ smaller than $\theta_{c3,4}$, light can be refracted at an external outcoupling angle of less than 90˚.

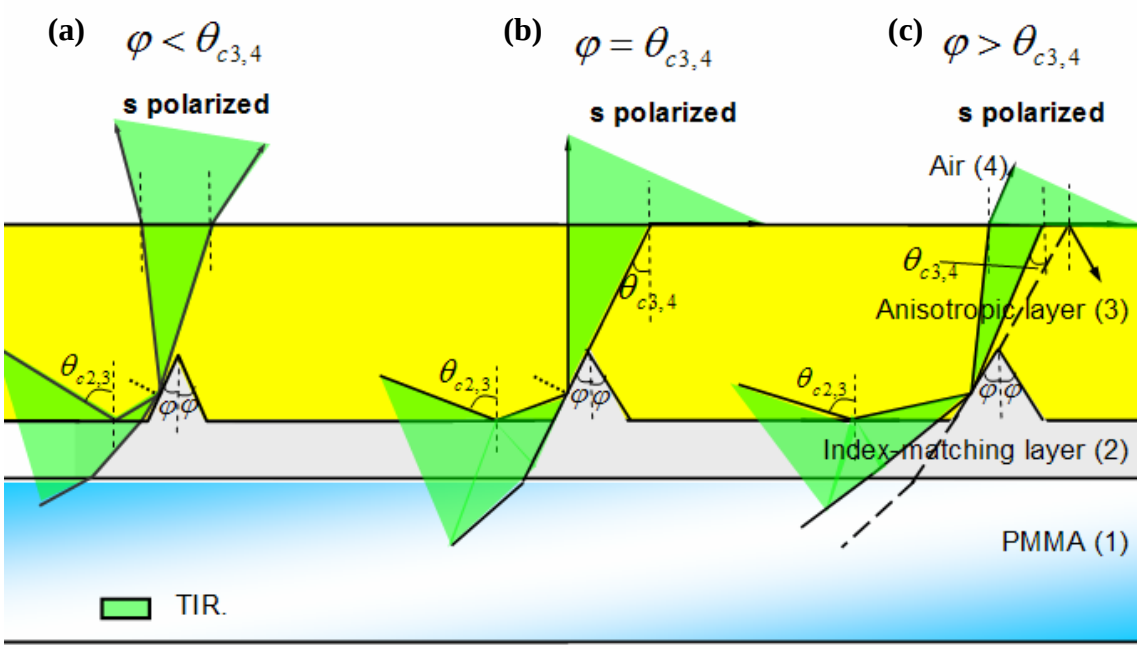

Fig. 5-2. Illustration of outcoupled s-polarized light due to selective T.I.R at the interface for different half top angles relative to the critical angle $\theta_{c3,4}$ of the anisotropic layer with respect to air:(a) $\varphi<\theta_{c3,4}$ (b) $\varphi=\theta_{c3,4}$ (c) $\varphi>\theta_{c3,4}$

5.3 Simulation

For further consideration to contrast ratio, angular distributions and efficiency, several issues were analyzed. An optical simulation and analysis program, Advanced System Analysis Program (ASAP), was used to simulate the polarized light by Monte Carlo ray tracing in birefringent material, as schematically shown in Fig. 5-3. Uniaxial birefringent materials, stretched Polyethylene terephthalate (PET) and Polyethylene Naphthalate (PEN), were used as an anisotropic layer, which were adhered on polymethyl methacrylate (PMMA) substrate by an index-matching glue. Furthermore, in order to analyze both s-polarized and p-polarized light, a polarizer

was built on the top of polarized backlight model. S-polarized light was analyzed when the direction of polarizer was parallel to the direction of micro grooves. P-polarized light was analyzed when the direction of polarizer was perpendicular to the direction of micro grooves.

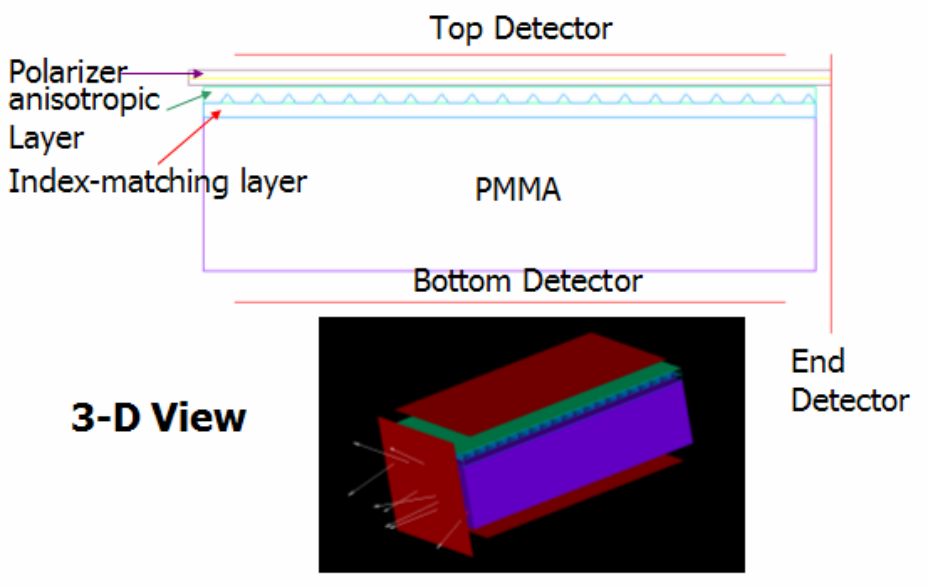

Fig. 5-3. Schematics of simulated polarized backlight model built by ASAP.

However, some issues affect the angular distribution, contrast ratio and luminance of extracted light. In the next section, these key issues will be concerned as followed:

(a) Index-mismatching of the coating layer

(b) Influence of vertex angles of micro grooves

(c) Influence of various substrates

5.3.1 Index-mismatching of the Coating Layer

The coating layer between anisotropic layer and PMMA substrate is not only an adhesive layer, but also an index-matching layer. Undesired T.I.R at the interface between the coating and PMMA will be present if the refractive index of the coating

layer is sufficiently smaller than the refractive index of PMMA. A reasonable refractive index of the coating layer should be ranged between the refractive index of PMMA and the extraordinary refractive index of anisotropic layer. In the polarized backlight, two anisotropic materials, Polyethylene terephthalate (PET) and Polyethylene Naphthalate (PEN), were analyzed. The parameters of two foils were listed as followed:

(i) PET: n_{PMMA}=1.49; $n_{o,PET}$=1.53; $n_{e,PET}$=1.71; vertex angle of groove=50°

(ii) PEN: n_{PMMA}=1.49; $n_{o,PEN}$=1.56; $n_{e,PEN}$=1.86; vertex angle of groove=50°

Contrast ratio of the polarized backlight model was analyzed at different refractive indices of index-matching layer. Contrast ratio is defined as the ratio of intensity of s-polarized to p-polarized light. For PEN foil, contrast ratio achieves 190 at perfectly matched n=1.56, whereas 160 at n=1.53 for PET foil, shown in Fig. 5-4.

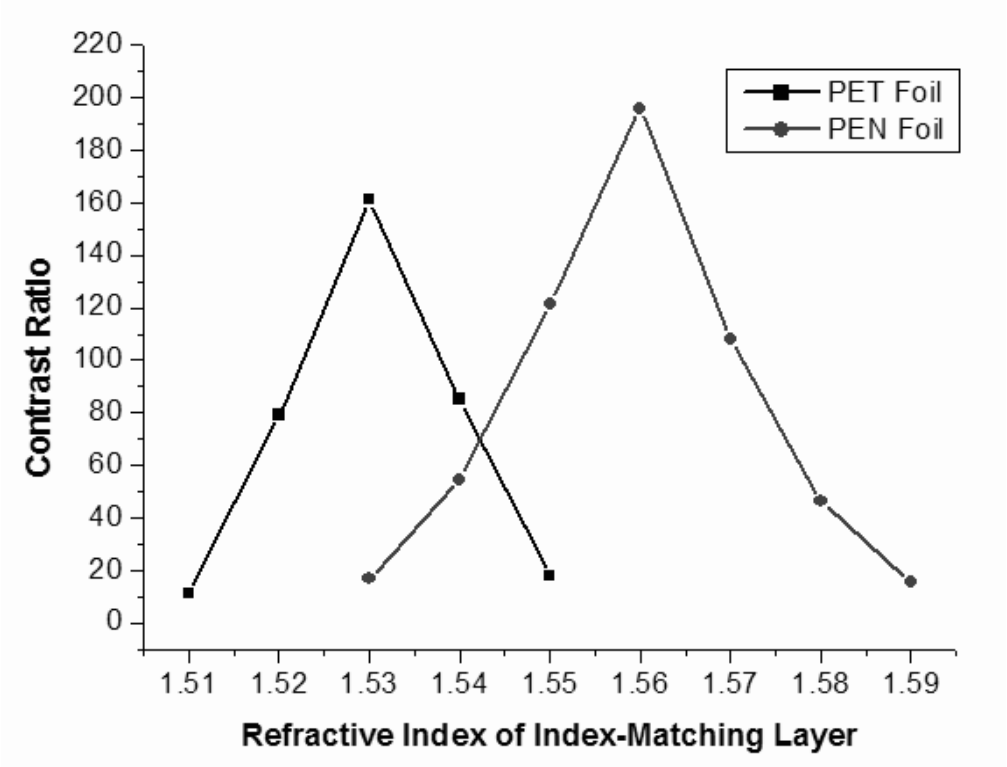

Fig. 5-4. Illustration of contrast ratio at different refractive index of index-matching layer. Contrast ratio achieves maximum at perfectly matched refractive index n=1.53 for PET foil, whereas n=1.56 for PEN foil.

5.3.2 Influence of Vertex Angles of Micro-grooves

As shown in Fig. 5-5, the angular distribution of the s-polarized light was related to the extracted angles θ_{max} and θ_{min}. According to geometric calculations, θ_{max} and θ_{min} can be derived from Snell's equations: $\theta_{max}=\sin^{-1}[n_e\times\sin(\varphi-\theta_{c3,4})]$ and $\theta_{min}=\sin^{-1}[n_e\times\sin(\theta_{c2,3+}\varphi/2-90^\circ)]$; where $\theta_{c2,3}$ and $\theta_{c3,4}$ denote the critical angles of the anisotropic layer with respect to the index-matching layer and air, respectively. Consequently, the emitted cones of the s-polarized light were determined by the vertex angle φ of grooves as well as the refractive indices n_e and n_o of the anisotropic layer. By assuming n_e= 1.71 and n_o=1.53, $\theta_{c2,3}$ and $\theta_{c3,4}$ were made equal to 63.4˚ and 39˚, respectively. To minimize θ_{min}, the vertex angle φ of grooves was made approximately equals to 50˚. Additionally, the θ_{max} of 20˚ of was obtained. Therefore, the outcoupled angular distributions range within ±20˚.

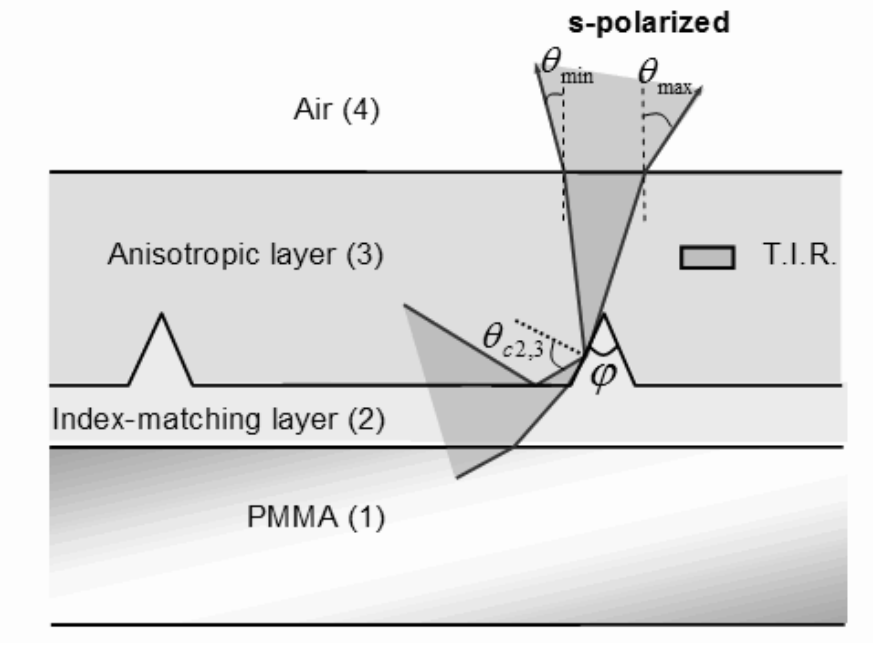

Fig. 5-5. Illustration of outcoupled s-polarized light due to selective T.I.R at interface of grooves in anisotropic layer.

The direction of extracted s-polarized light was controlled by inclined surface

of micro grooves. Therefore, angles of micro grooves determine angular distributions of polarized backlight. Polyethylene terephthalate (PET): The parameters of micro grooves were listed below.

Depth of grooves= 56.5 μm; Pitch of grooves= 200 μm

The angle of micro-groove was tuning from 30° to 90°.

The angular distribution was shifted when the vertex angle of groove was increased as shown in Fig. 5-6. When the angle of groove was tuned from 30° to 45°, the angle of s-polarized light was distributed in the negative angle direction. When the angle of groove was tuned to be 50°, the angle of s-polarized light was distributed in the normal direction. When the angle of groove was tuned from 60° to 90°, the angle of s-polarized light was distributed in the positive angle direction.

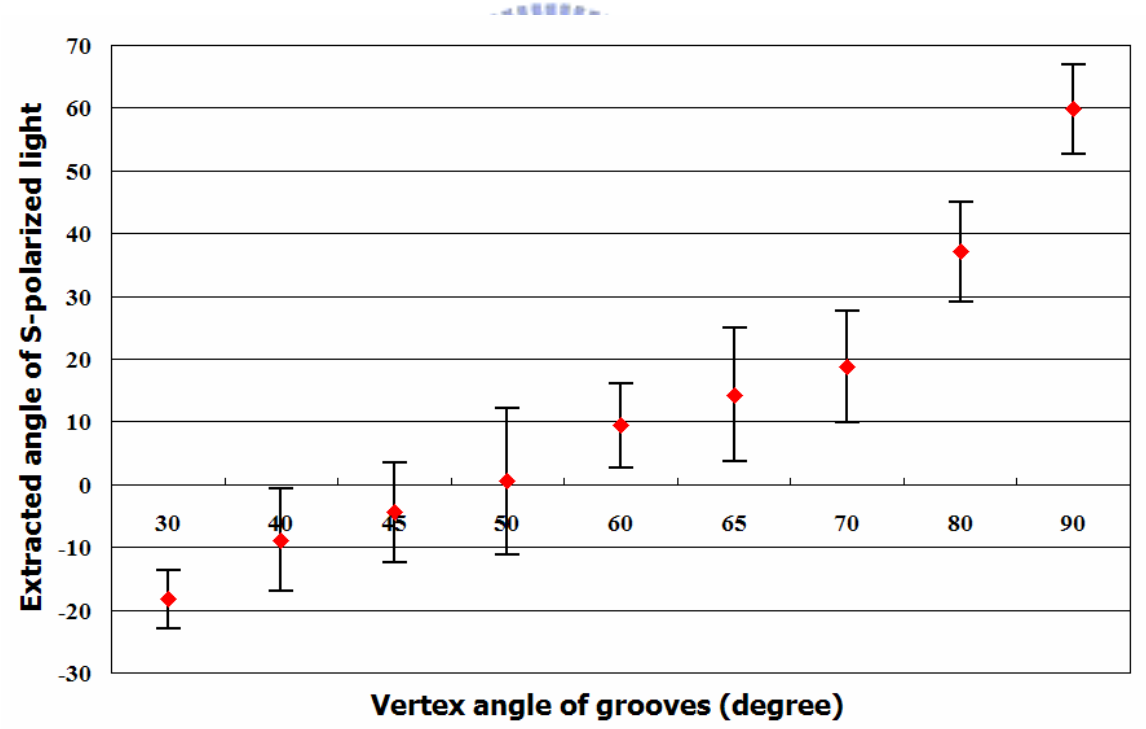

Fig. 5-6. Angular distribution of S-polarized light versus vertex angle of grooves in PET foil. The bars represent the amount of angular ranges at FWHM.

Additionally, the bars represent the amount of angular ranges at FWHM (Full Width Half Maximum) as shown in Fig. 5-6. As the angle of groove was increased,

the angular distribution of s-polarized light was shifted toward the positive angular direction.

Similarly, by using Polyethylene Naphthalate (PEN) foil, the polarized backlight model was simulated by the following parameters of micro grooves.

Depth of grooves= 56.5 μm

Pitch of grooves= 200 μm

The angle of micro-groove was tuning from 30° to 90°.

As shown in Fig. 5-7, the angular distribution was shifted when the vertex angle of groove was increased.

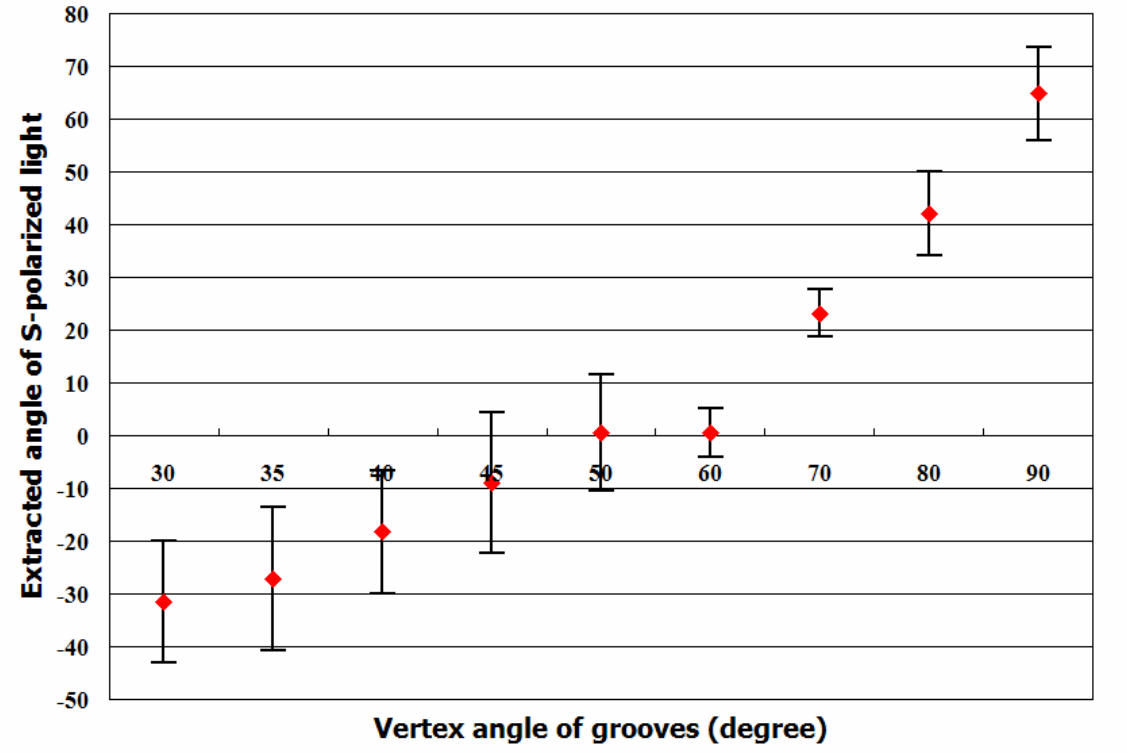

Fig. 5-7. Angular distribution of S-polarized light versus vertex angle of grooves in PEN foil.

When the angle of groove was tuned from 30° to 45°, the angle of s-polarized light was distributed in the negative angle direction. When the angle of groove was tuned

from 50° to 60°, the angle of s-polarized light was distributed in the normal direction. When the angle of groove was tuned from 70° to 90°, the angle of s-polarized light was distributed in the positive angle direction. As the angle of groove was increased, the angular distribution of s-polarized light was shifted toward the positive angular direction.

From the simulated results shown in Figs. 5-5 and 5-6, the vertex angles of micro-grooves by using PET and PEN foils were eventually chosen as 50°. This is mainly attributed to the angular distribution of extracted light occurring at the normal viewing while making the vertex angle equal to 50°. In order to describe the angular distribution of extracted light in details, we demonstrated the angular distributions and inclined angular cross-sections of extracted s-polarized light at perfectly matched index for PEN and PET foils, respectively, as shown in Fig. 5-8. The vertex angle of grooves is 50°. The angular profiles are plotted as a function of inclination angles, which are ranging from -90° and 90°, with respect to the normal viewing direction. Most of s-polarized light is distributed between the inclination angle of -30° and 30° for PEN foil while -20° and 20° for PET.

(a)

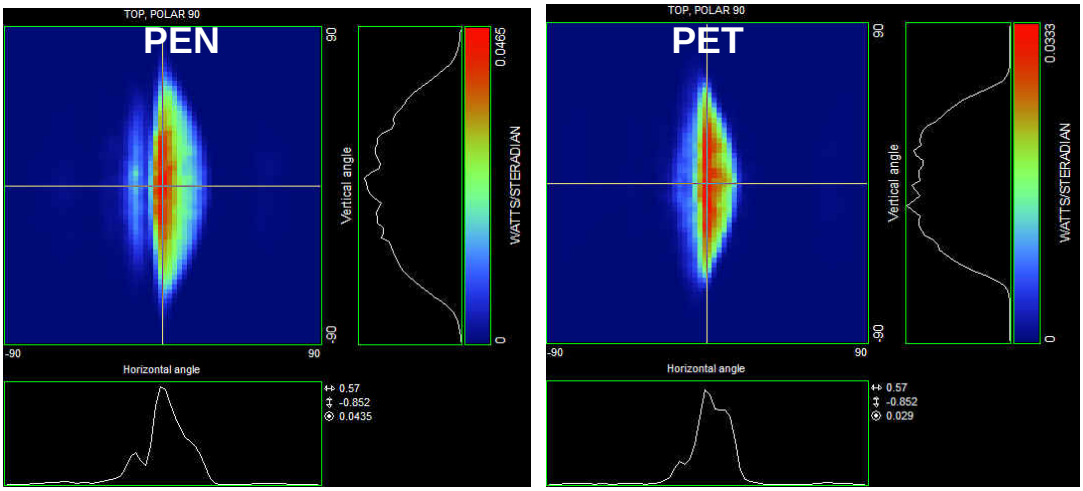

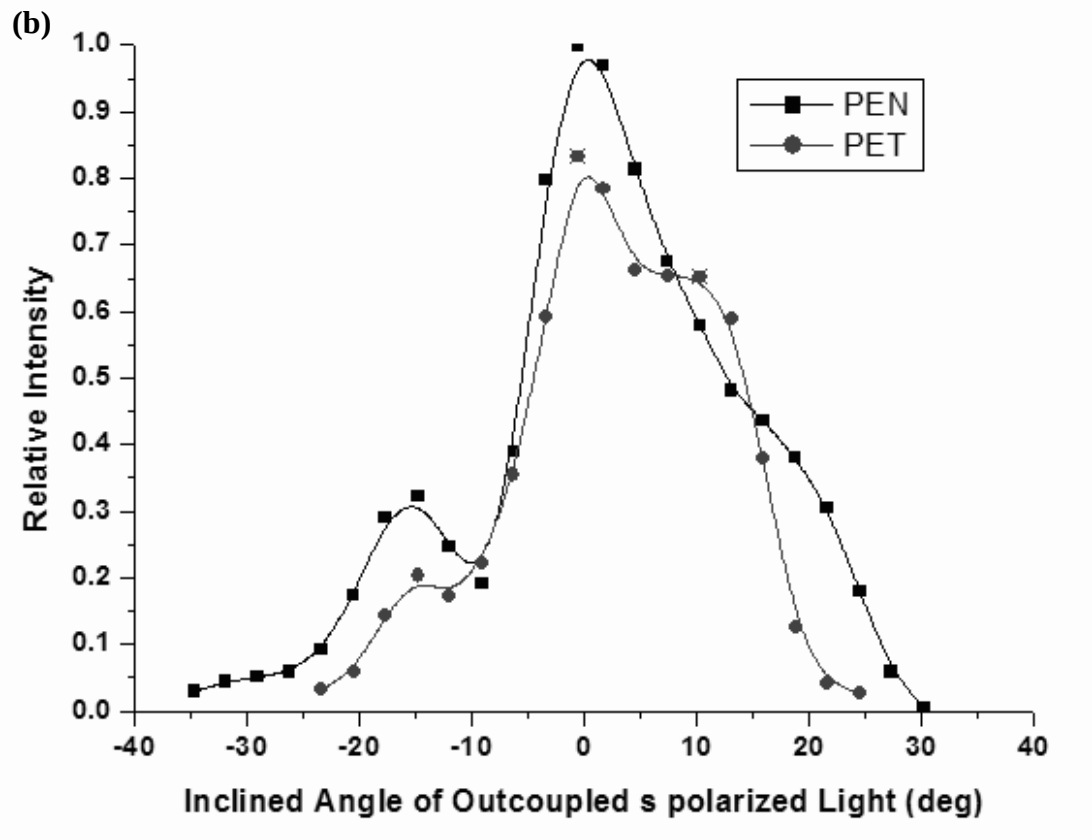

Fig. 5-8. (a) Angular distributions and (b) Inclined angular cross-sections of extracted s-polarized light at perfectly matched index for PEN and PET foils.

5.3.3 Influence of Various Substrates

In the previous section, PMMA substrate (n=1.49) was used in simulation. Influence of various substrates, such as PC substrate (n=1.585), needs to be further evaluated. As shown in Fig. 5-9, by using PEN foil, angular distributions with PC substrates at FWHM (20°) were narrower than those with PMMA substrates (30°). The narrower angular distribution with PC substrate is mainly attributed to the less refractive index differences.

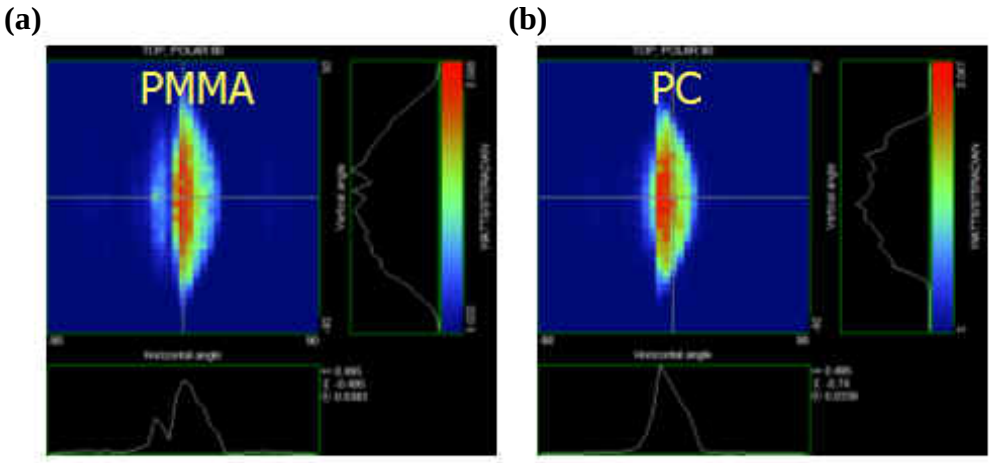

Fig. 5-9. Angular distributions of s-polarized light with (a) PMMA substrate (b) PC substrate while groove angle=50˚ and perfectly index-matched in PEN foils.

Compared with PET foil, stretched PEN foil demonstrates higher contrast ratio of s-polarized to p-polarized light due to large difference of refractive indices. ($\Delta n=n_{e,PEN} - n_{o,PEN}=0.3$, $\Delta n=n_{e,PET} - n_{o,PET}=0.18$) Additionally, PEN demonstrates a wider angular distribution than PET due to the large birefringence. Most of s-polarized light is distributed between the inclination angle of -30˚ and 30˚ for PEN foil while -20˚ and 20˚ for PET. A smaller critical angle is presented at the interface of grooves for PEN, thus, broadening the angular distribution on the outcoupled plane. In simulation, when the ordinary refractive index $n_o=1.56$ of PEN foil is perfectly matched the refractive index of glue layer, flux of p-polarized light is expected to achieve a minimum, whereas for PET foil perfectly matched at $n_o=1.53$. Therefore, contrast ratio of s-polarized light to p-polarized light achieves a maximum.

However, the mismatched indices between the anisotropic foil and the glue layer cause increasing amount for p-polarized light due to Fresnel surface reflection at the interface,[7] but not obviously for s-polarized light, thus, degrades contrast ratio. To retain contrast ratio of higher than 80, the refractive index of the glue layer can be mismatched within ±0.015 for PEN foil, whereas ±0.01 for PET foil. Therefore, PEN foil provides higher tolerances in mismatched refractive indices compared with PET

foil.

5.4 Fabrication

There were two approaches to fabricate micro grooves on anisotropic foils: micro-machining and embossing. Fabrication procedures were as the flow chart in Fig. 5-10.

(i) Flatness was an important concerning issue in fabrication. A vacuum system will replace the traditional adhesive due to flatness concern. Porous Aluminum was used as the stage of vacuum system. Anisotropic foil was tightly attached on the surface of Aluminum after the pump was switched on. Then, anisotropic foil was flattened and micro-machined by diamond cutting. The vertex angle and depth of the grooves are 50° and 56.5 μm, respectively. The pitch of the grooves is 200 μm.

(ii) Index-matched glue was filled between PMMA substrate and anisotropic foil. Then, UV curing was done.

(iii) Vacuum condition was broke. Prototype of polarized backlight was removed from the vacuum stage.

For the purpose of mass replication of anisotropic foil with micro-grooves, the embossing/extrusion technology can be further applied. By using the embossing/extrusion fabrication, only step (i) was replaced by embossed anisotropic foils.

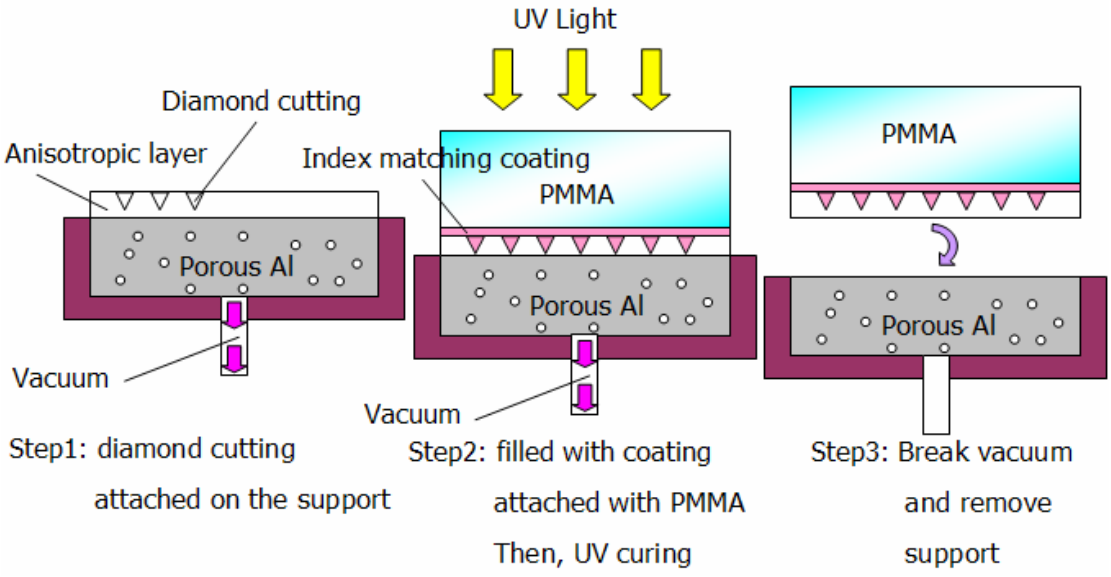

Fig. 5-10. Fabrication process of polarized backlights.

5.5 Measurement

Because PEN foil exhibited higher contrast ratio and wider angular distribution compared with PET foil, the prototypes of polarized backlight with PEN foil was fabricated and measured. The polarized backlight module was side-illuminated by a cold-cathode fluorescent lamp (CCFL). Angular distributions of emitting light from the backlight module were measured by an EZcontrast 160 measuring system, which is schematically shown in Fig. 5-11. To determine contrast ratio of s-polarized light to p-polarized light, a polarizer was placed between the backlight and detector as shown in Fig. 5-11, so that the transmission axis of polarizer could be rotated to be parallel or perpendicular to the extraordinary axis of birefringent layer. In addition, the brightness intensities in various positions (closer to the lamp or far from the lamp) can be measured to determine uniformity of polarized backlights. Figs. 5-12(a) and (b) demonstrated the angular distributions of s-polarized and p-polarized light, respectively, where the angular distributions were plotted as a function of azimuth angle, ϕ, ranging from 0° to 360°, and the inclination angle, θ, ranging from 0° to 80°.

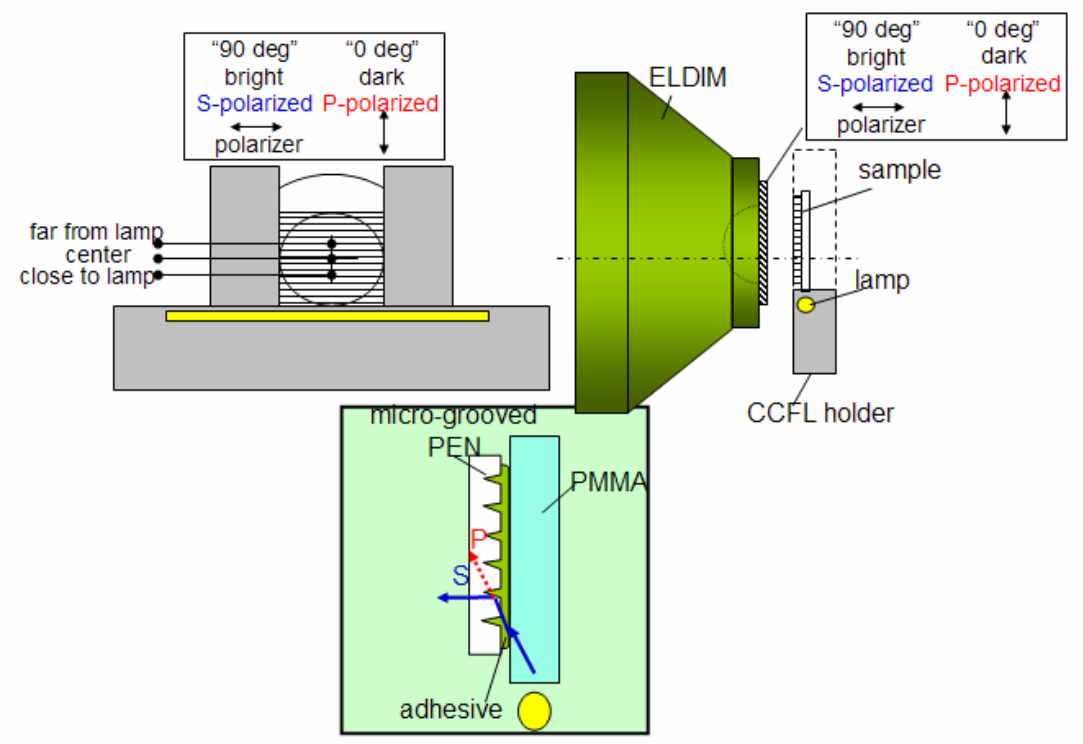

Fig. 5-11 Measurement set up of polarized backlight.

Peak intensity is 456 cd/m^2 for s-polarized light while 96 cd/m^2 for p-polarized light. Most s-polarized light is distributed between the inclination angle of -30° and 30°. P-polarized light is distributed in large inclination angles. Fig. 5-12(c) depicts contrast ratio of s-polarized light to p-polarized light. The peak contrast ratio can achieves 64.

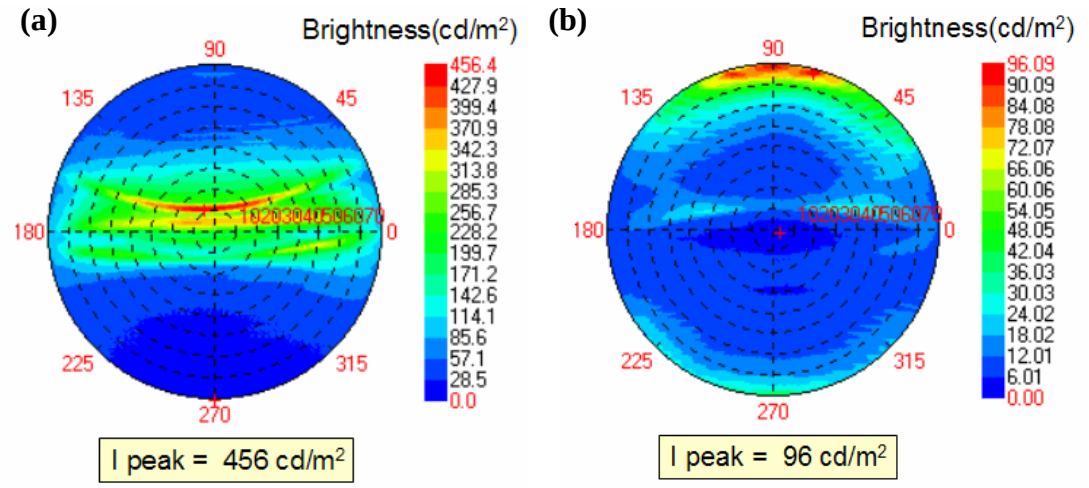

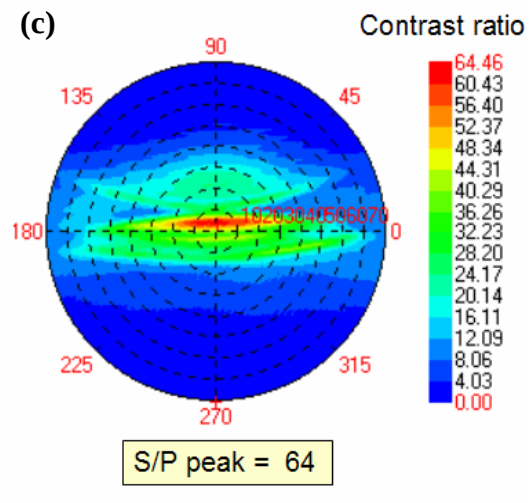

Fig. 5-12. Measured angular profiles of (a) s-polarized light (b) p-polarized light and (c) Contrast ratio of s-polarized to p-polarized light.

Fig. 5-13 (a) and (b) demonstrated luminance profiles of S-polarized light and P-polarized light of polarized backlight, which was fabricated by micro machining.

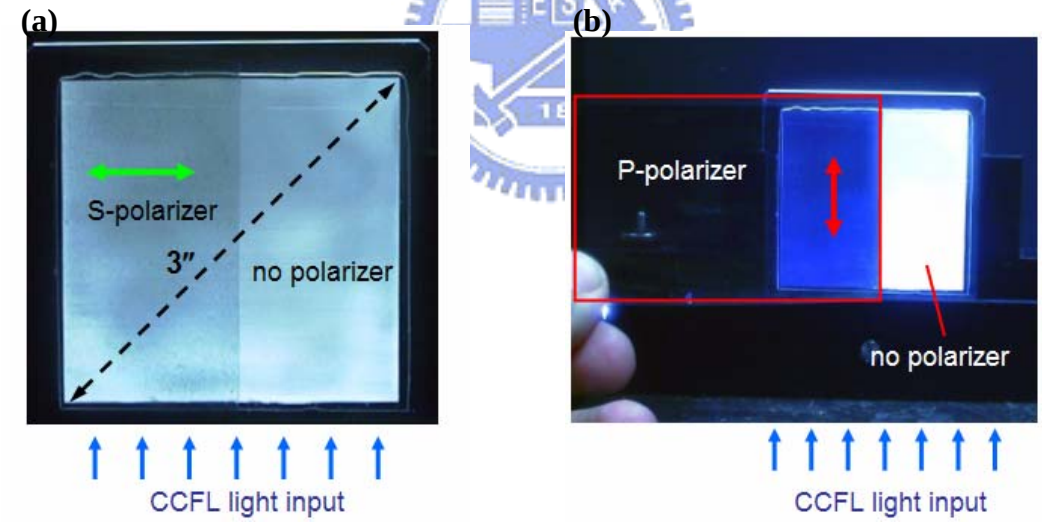

Fig. 5-13. Luminance profiles of (a) S-polarized light and (b) P-polarized light. A polarizer was rotated to observe S-polarized and P-polarized light, respectively.

From the measured results, it is clear that s-polarized light significantly dominates the extracted light of polarized backlight module. However, from the measured results, contrast ratio is lower than our designed value because of the

presence of dust and air bubbles during the process of micromachining anisotropic foil and the index-matching glue. Due to scattering light occurred at the surfaces of micro-grooves, contrast ratio of s-polarized to p-polarized light is not high enough yet. We expect that the contrast ratio can be further enhanced when the surface smoothness of the micro-grooves is improved.

5.5.1 Uniformity

Additionally, luminous intensity was sequentially measured from a position of 8 mm away from light source (close to light source) to a position of 52 mm away from light source (far away from light source).

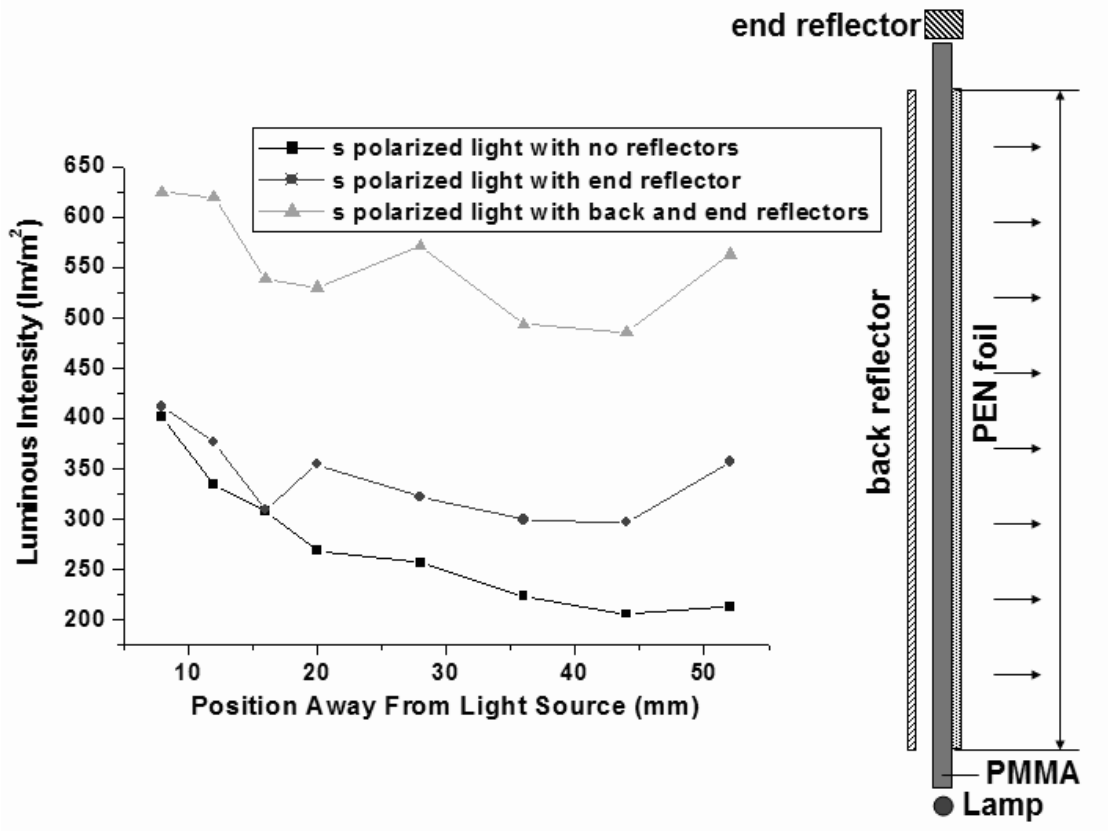

Fig. 5-14. For PEN foil adhered on the substrate of PMMA, luminous intensity versus position from light source for polarized backlight with PEN foil. Curves with square, round, and triangle marks illustrate luminous intensity of s-polarized light with no reflectors, diffuse end reflector only, and both back and end reflectors, respectively.

Curves with square, round, and triangle marks illustrate luminous intensity of s-polarized light with no reflectors, diffuse end reflector only, and both back and end reflectors, respectively, which is shown in Fig. 5-14. With both back reflector and end reflector, maximum and minimum of luminous intensity are 625 and 500 lm/m^2, respectively. Uniformity can therefore achieve 80%.

5.5.2 Gain of Efficiency

In order to evaluate gain of efficiency of polarized backlight, efficiency was measured by following procedures shown in Fig. 5-15.

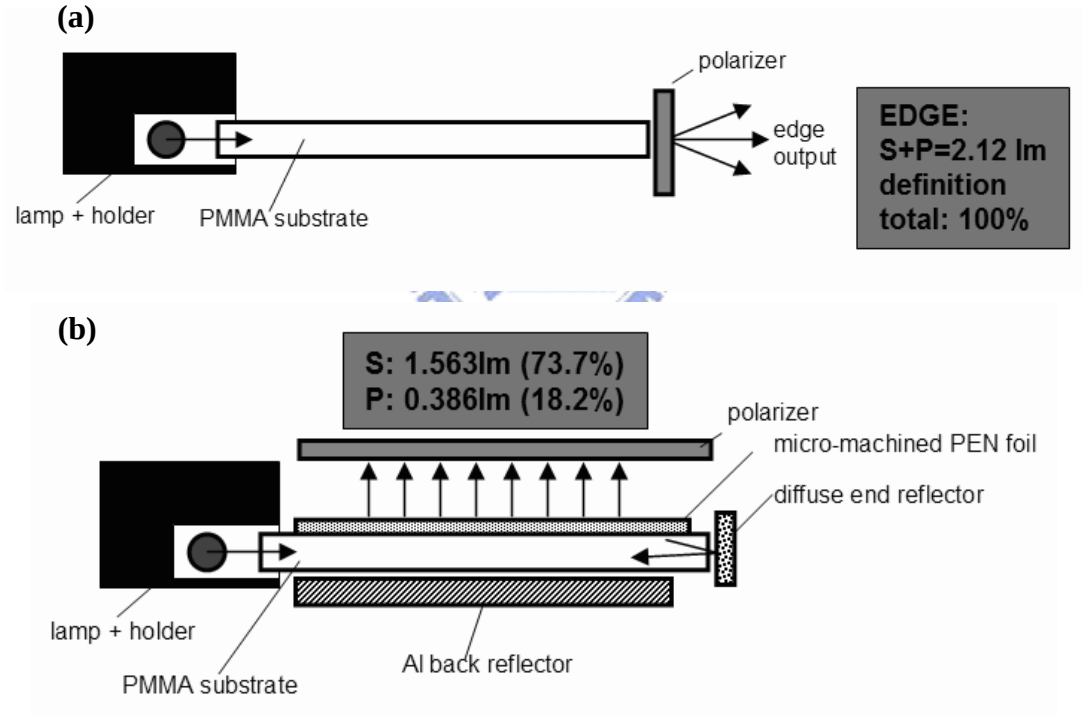

Fig. 5-15. Measurement set up of flux by (a) clear PMMA (b) polarized backlight with both back and end reflectors.

Total input flux was measured at the end of a clear PMMA. Theoretically, all the rays were T.I.R in the lightguide until transmitting through the end. Therefore, total input flux was 2.12 lm. Then, fluxes of s-polarized and p-polarized light were sequentially

measured to be 1.56 and 0.39 lm, respectively, from the outcoupled plane. Input fluxes of s-polarized and p-polarized light were assumed to be equally 0.975 lm. ((1.56 lm+0.39 lm)/2=0.975 lm) Outcoupled energy was totally 92% of input flux. The rest 8% flux was lost in reflectors and lamp. Therefore, an efficiency gain factor of 1.6 was achieved for s-polarized light. (gain factor = 1.56 lm/0.975 lm = 1.6)

5.6 Discussion

Although the polarized backlight with PEN foil exhibits high gain in efficiency, some issues, such as collimated angular distribution and backward polarized light emission, need to be discussed more detailedly and feasible solutions to these issues will be proposed in the following section.

5.6.1 Broadening Angular Distribution

According to the measurement, for the polarized backlight with PEN foil, most of s-polarized light was distributed between the inclination angle of -30˚ and 30˚. The polarized backlight that presents a narrow angular profile is suitable for collimated angular application but constrained in wide viewing illumination. In order to broaden the angular distributions, grooves of various vertex angles in the birefringent foils were utilized to combine slightly shifted cones of s-polarized light, which is shown in Fig. 5-16.

A combination of 35˚, 50˚ and 60˚ vertex angles was modeled and eventually chosen because vertex angles of grooves were proper to be micro-machined. In addition, less oscillation was caused in the luminous intensity distribution. For ϕ'=90˚-270˚ cross section, Fig. 5-17 depicts the angular distributions for 50˚ of vertex angles and combined 35˚, 50˚ and 60˚ of grooves, respectively. Compared with vertex angle of 50˚, the angular distribution of s-polarized light was distributed between the

inclination angle of -45˚ and 45˚, thus, broadening by a factor of 1.5.

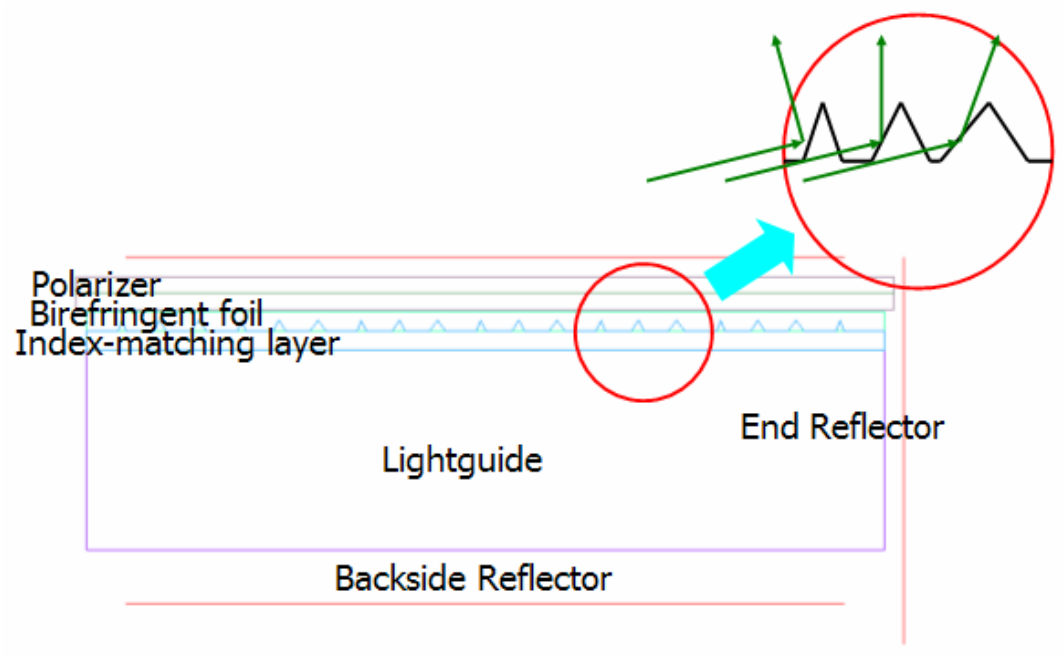

Fig. 5-16. Schematics of combined grooves with various angles in the birefringent foil.

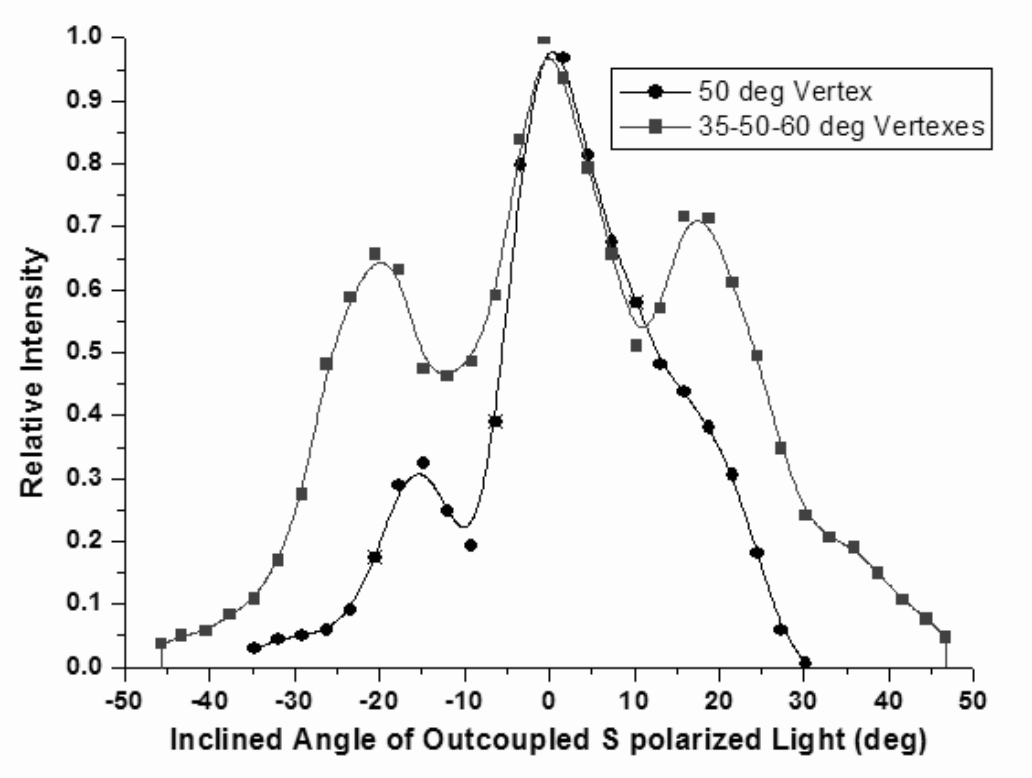

Fig. 5-17. For φ'=90˚-270˚ cross section, angular profiles while the vertex angles of grooves are 50˚ and combined 35˚, 50˚ and 60˚, respectively.

5.6.2 Backward Polarized light Emission

As shown in Fig. 5-18(a), because refraction of s-polarized light occurs at the grooves, part of s-polarized light is emitted from the backside of lightguide. The angular distributions of lost s-polarized light were measured from the backside of the lightguide, as shown in Fig. 5-18(b).

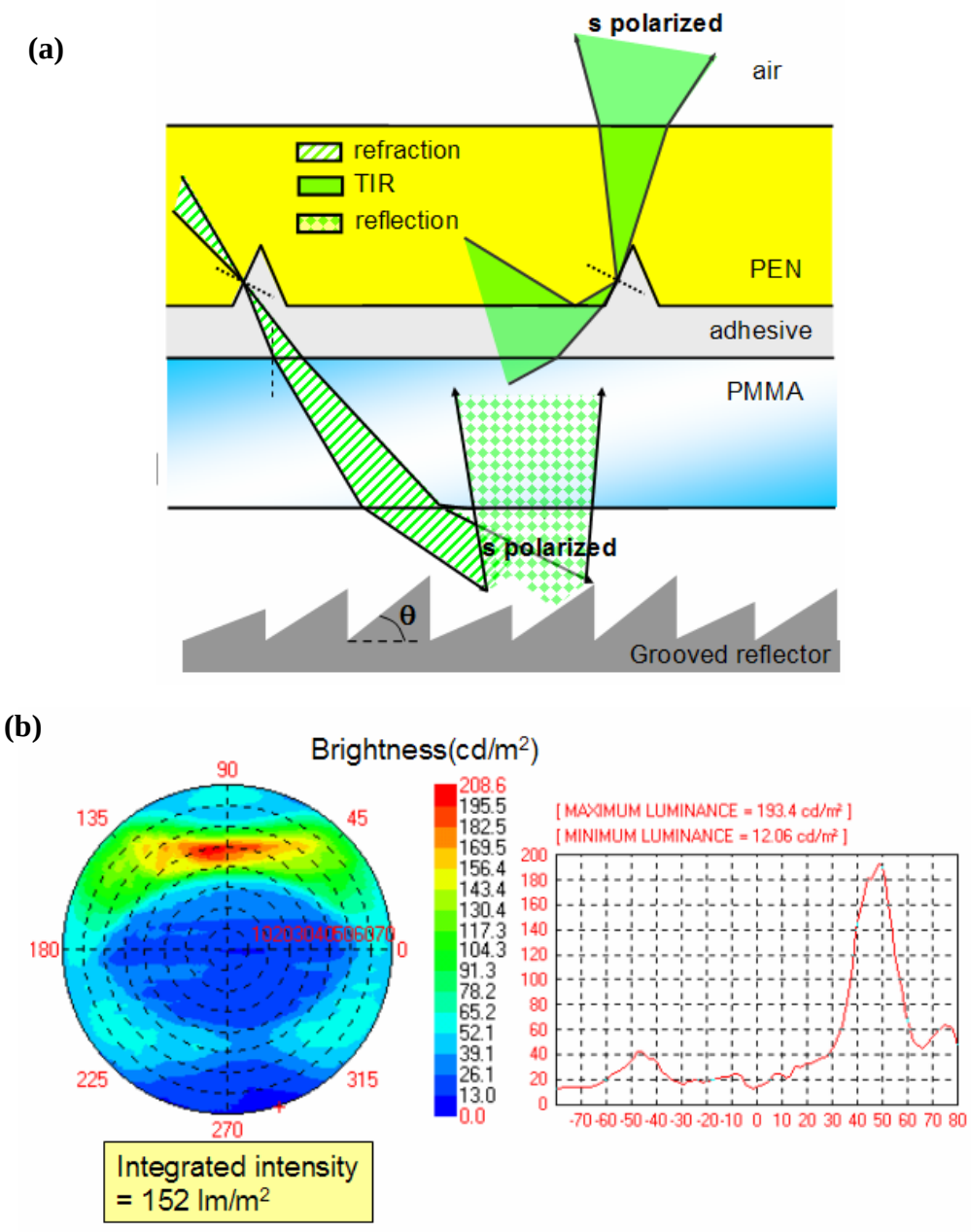

Fig. 5-18. (a) Refraction of s-polarized light at the micro grooves (b) Measured angular profiles of s-polarized light from the backside of the lightguide.

Most of s-polarized light is distributed between 30˚ and 70˚. In convention, a smooth specular reflector placed below the lightguide was first considered to recycle lost s-polarized light from the back plane of lightguide. In order to more efficiently redirect and recycle emitted s-polarized light from the backside of lightguide toward the normal viewing direction, a specular reflector was replaced by a grooved reflector. A grooved reflector of inclined angles from 20˚ to 40˚ in gradient was eventually chosen because a smooth luminous intensity distribution was obtained within the viewing cones of ±40˚. Fig. 5-19 plots the dependence of relative intensity on various viewing angles for using a specular reflector and a grooved reflector, respectively. The redirected s-polarized light from the grooved reflector resulted in compensated angular cones within the viewing angles of ±40˚. In addition, the luminous intensity was increased by a factor 1.3.

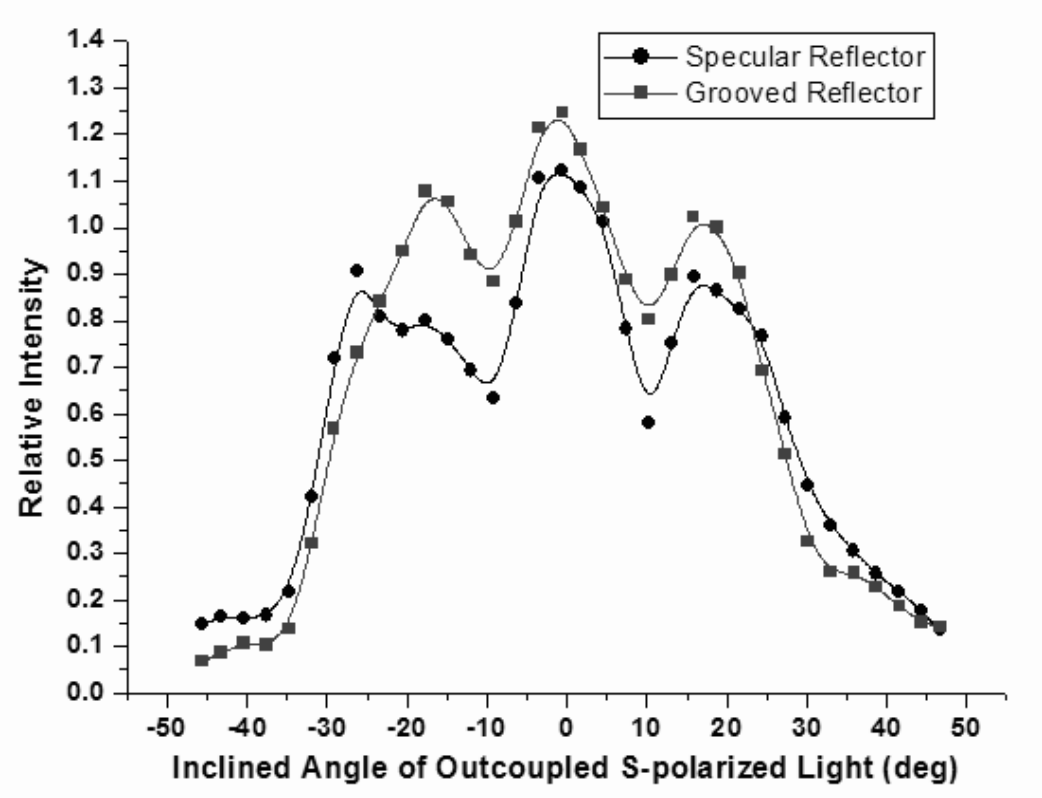

Fig. 5-19. Dependence of relative intensity on various viewing angles for using a smooth specular reflector and a grooved reflector, respectively.

5.7 Summary

A polarized backlight based on selective T.I.R at the interface of micro-grooves was demonstrated. By using micro-machined PEN foil, extracted s-polarized light is in a cone of $\pm 30^{\circ}$ around the surface normal, while p-polarized stray light is in large inclination angles. Contrast ratio in normal viewing direction can be as high as 64. Some concerned issues, such as collimated angular distribution and backward polarized light emission, can be improved by using combined grooves in the birefringent foil and the grooved reflector. Additionally, polarized backlights with end and back reflectors provide luminous uniformity of higher than 80%. 1.6 of gain in efficiency is obtained aiming for high efficiency LCD illumination. As a result, less complexity, thinner thickness and higher brightness of LCDs can be achieved.

5.8 References

[1] H. Jagt, H. Cornelissen, D. Broer, C. Bastiaansen, Society Information Display (SID) Digest, p.1236 (2002).

[2] H. Jagt, H. Cornelissen, D. Broer, Journal of SID, p.209 (2002)

[3] H. Cornelissen, H. Jagt, D. Broer, C. Bastiaansen, K. W. Chien, International Display Workshop (IDW) Digest, p.659 (2004)

[4] E. Hecht, Optics, Addison-Wesley, 2nd edition, p. 84 (1987)

[5] F. J. Pedrotti, L. S. Pedrotti, Introduction to Optics, Prentice Hall London, 2nd edition, p.38 (1993)

[6] H. Jagt, *Polymeric Polarisation Optics for Energy Efficient Liquid Crystal Display Illumination*, University Press Facilties, Eindhoven, The Netherlands, p.114 (2001)

[7] G. R. Fowles, Introduction to Modern Optics, Holt, Rineheart, and Winston, New York, 2nd edition, p.168.